Available at: http://publications.ictp.it IC/2010/055

United Nations Educational, Scientific and Cultural Organization
and
International Atomic Energy Agency

THE ABDUS SALAM INTERNATIONAL CENTRE FOR THEORETICAL PHYSICS

EARTHQUAKE ENERGY DISTRIBUTION ALONG THE EARTH SURFACE AND RADIUS

P. Varga[1]
Geodetic and Geophysical Research Institute, Seismological Observatory, Hungary,

F. Krumm
Geodätisches Institut, Universität Stuttgart, Germany,

F. Riguzzi
Istituto Nazionale di Geofisica e Vulcanologia, Roma, Italy,

C. Doglioni
Dipartimento di Scienze della Terra, Università Sapienza, Roma, Italy,

B. Süle
Geodetic and Geophysical Research Institute, Seismological Observatory, Hungary,

K. Wang
Geodätisches Institut, Universität Stuttgart, Germany

and

G. F. Panza
Dipartimento di Geoscienze, Università degli Studi di Trieste, Trieste, Italy
and
The Abdus Salam International Centre for Theoretical Physics, Trieste, Italy.

MIRAMARE – TRIESTE

July 2010

[1] Corresponding author, varga@seismology.hu

Abstract

The global earthquake catalog of seismic events with $M_W \geq 7.0$, for the time interval from 1950 to 2007, shows that the depth distribution of earthquake energy release is not uniform. The 90% of the total earthquake energy budget is dissipated in the first ~30km, whereas most of the residual budget is radiated at the lower boundary of the transition zone (410 km - 660 km), above the upper-lower mantle boundary. The upper border of the transition zone at around 410 km of depth is not marked by significant seismic energy release. This points for a non-dominant role of the slabs in the energy budged of plate tectonics.

Earthquake number and energy release, although not well correlated, when analysed with respect to the latitude, show a decrease toward the polar areas. Moreover, the radiated energy has the highest peak close to (±5°) the so-called tectonic equator defined by Crespi et al. (2007), which is inclined about 30° with respect to the geographic equator. At the same time the presence of a clear axial co-ordination of the radiated seismic energy is demonstrated with maxima at latitudes close to critical (±45°). This speaks about the presence of external forces that influence seismicity and it is consistent with the fact that Gutenberg-Richter law is linear, for events with M>5, only when the whole Earth's seismicity is considered. These data are consistent with an astronomical control on plate tectonics, i.e., the despinning (slowing of the Earth's angular rotation) of the Earth's rotation caused primarily by the tidal friction due to the Moon. The mutual position of the shallow and ~660 km deep earthquake energy sources along subduction zones allows us to conclude that they are connected with the same slab along the W-directed subduction zones, but they may rather be disconnected along the opposed E-NE-directed slabs, being the deep seismicity controlled by other mechanisms.

1. Introduction

One of the most significant physical characteristics of earthquakes is the energy they radiate. Probably this is the reason why this problem attracted the attention of scientists at the very beginning of the development of modern seismology. Presumably Mendenhall was the first scientist who estimated the energy of earthquake waves and got for the Charlston (1886) and Tokyo (1887) earthquakes the values $2.5 \cdot 10^{13}$ Joule and $3.3 \cdot 10^{14}$Joule, respectively (Howell, 1990). Milne in 1886 discussed on a theoretical base the problem of earthquake energy. Kövesligethy (1897; 1903) calculated the energy of seismic events which occurred in 1897 and 1903. He assumed that all displacements of the rotation axis of the Earth are convertedinto seismic energy and therefore significantly overestimated the energy of earthquakes. A realistic estimate of earthquake energy ($E \sim 1.75 \cdot 10^{17}$ Joule) was done in 1910 by Reid for the case of 1906 San Francisco earthquake and somewhat later for some other seismic events on the basis of the work produced by displacing the geological masses (Reid, 1912). Other early attempts to determine seismic energy are given in the book by Sieberg (1923). Due to the fact that most of the recorded seismic energy in the case of teleseismic events is represented by surface waves the first attempts by Galitzin (1915) and Klotz (1915) to use seismograms of the Pamir earthquake of 1911, February 18 ($M_S = 7.6$ according to Abe and Noguchi, 1983) was based on the analysis of Rayleigh waves and gave the values of 6×10^{16} Joule and 7×10^{16} Joule, respectively. The method by Galitzin was improved later on by Jeffreys (1923). In the thirties of the 20th century, Richter developed a magnitude scale for local earthquakes of California (Richter, 1935). This approach after WW II has been generalized to magnitudes of teleseismic events with the use of body waves (m_b) and surface waves (M_S). The main problem in the use of these magnitude values is that they saturate in case of strong earthquakes: in case body waves if $m_b \geq (5.5\text{-}6.0)$ and in case of surface waves if $M_S \geq 7.0$.

Gutenberg and Richter (1956) found for surface waves that $\log E_S = 1.5M_S + 4.8$. Hanks and Kanamori (1979) introduced instead of M_S the momentum magnitude M_W that does not saturate and obeys a similar equation $\log E_W = 1.5M_W + 4.8$ (E_S and E_W are in Joule). The magnitude based earthquake energy quantifies only the radiated energy, which does not always coincides with the total amount of energy released by a seismic source.

The main goal of the present study is to investigate the distribution of the radiated seismic energy, E_W, at the Earth surface and its depth dependence. Due to the fact that 90%-95% of the total earthquake energy is produced by seismic events with $M_W \geq 7.0$ only these large events are considered in this study. This choice guarantees a satisfactory level of completeness and quality of the earthquake catalog considered, for the time interval from 1950 to 2007 and makes it worthwhile to compare the distribution of discharged seismic energy with the distribution of the number of earthquakes $M_W \geq 7.0$ and with the surface distribution of the main linear tectonic structures.

2. The earthquake catalog

The completeness analysis of the available global earthquake list shows that, during the 20th century, it can be considered statistically complete for the events $M_W \geq 7.0$ (Kosobokov, 2004). For the needs of our study an earthquake catalog of great events ($M_W \geq 7.0$) has been compiled starting from the Centennial catalog, a global catalog of locations and magnitudes of instrumentally recorded large earthquakes (Engdahl and Villaseñor, 2002), assembled by combining existing catalogs, reducing all available magnitudes for each earthquake to a common, corrected magnitude and relocating the earthquakes with available arrival time data. The Centennial catalog extends from 1901 to April 2002 and it can be considered statistically complete for magnitudes $M_W \geq 7.0$. To expand the time span, we have added all the events with $M_W \geq 7.0$ from the USGS/NEIC global catalog. The updated dataset consists of 1719 events with $M_W \geq 7.0$, from 1901 to September 2007. In order to obtain uniform magnitude values in the depth interval from the surface down to 700 km, the M_W values are corrected according to the procedure described in Herak et al. (2001).

The distribution of the number of events, normalized with respect to latitude dependent area, per latitude classes shows that the polar regions are not affected by seismic activity, the maximum number of events falls in the range $10°\text{S} < \text{Latitude} \leq 0°$, 65% of the events falls in the range

30°S < Latitude ≤ 30°N and 28% of the events occurs at the middle latitudes of the northern hemisphere.

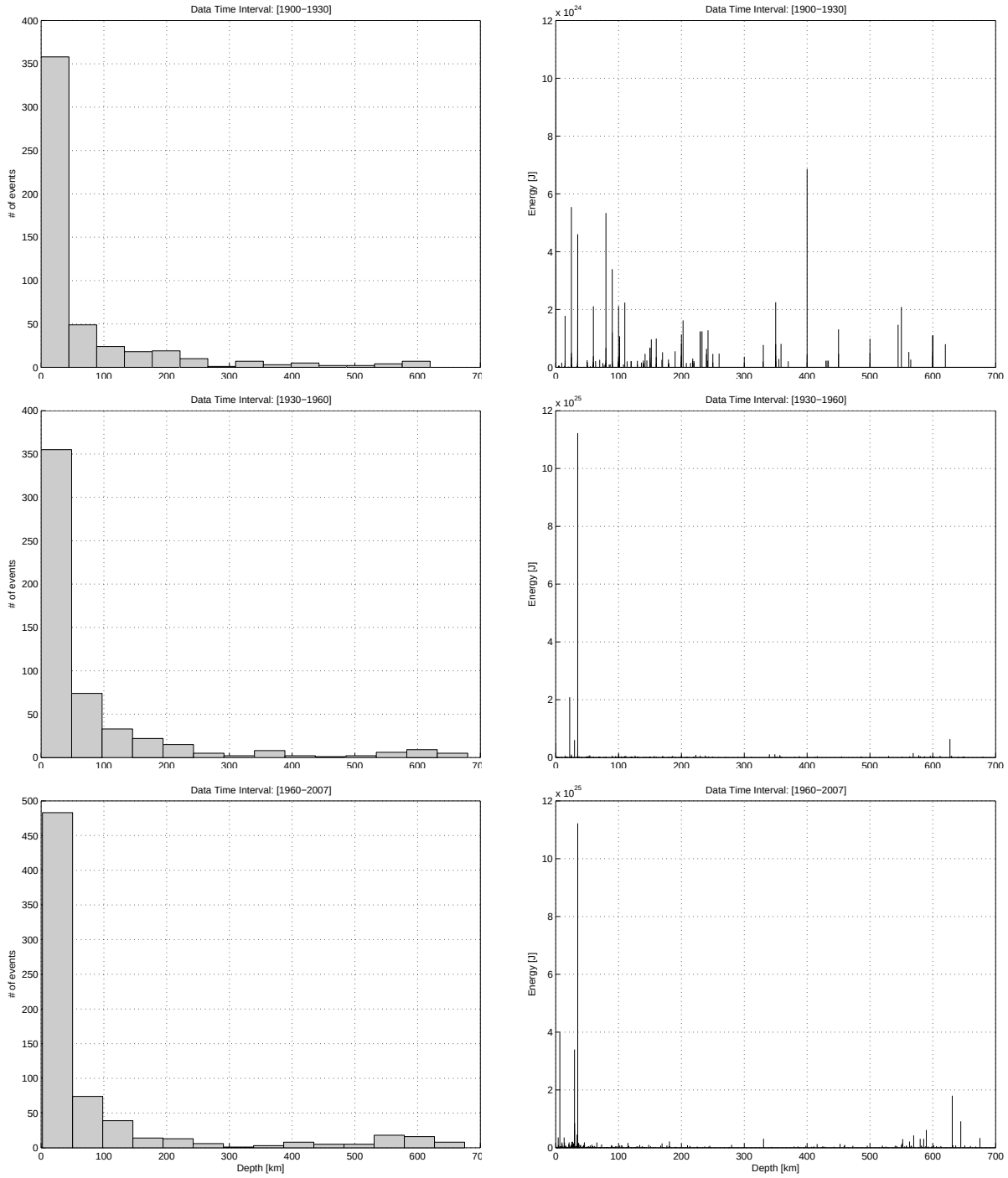

Figure 1a: along radius

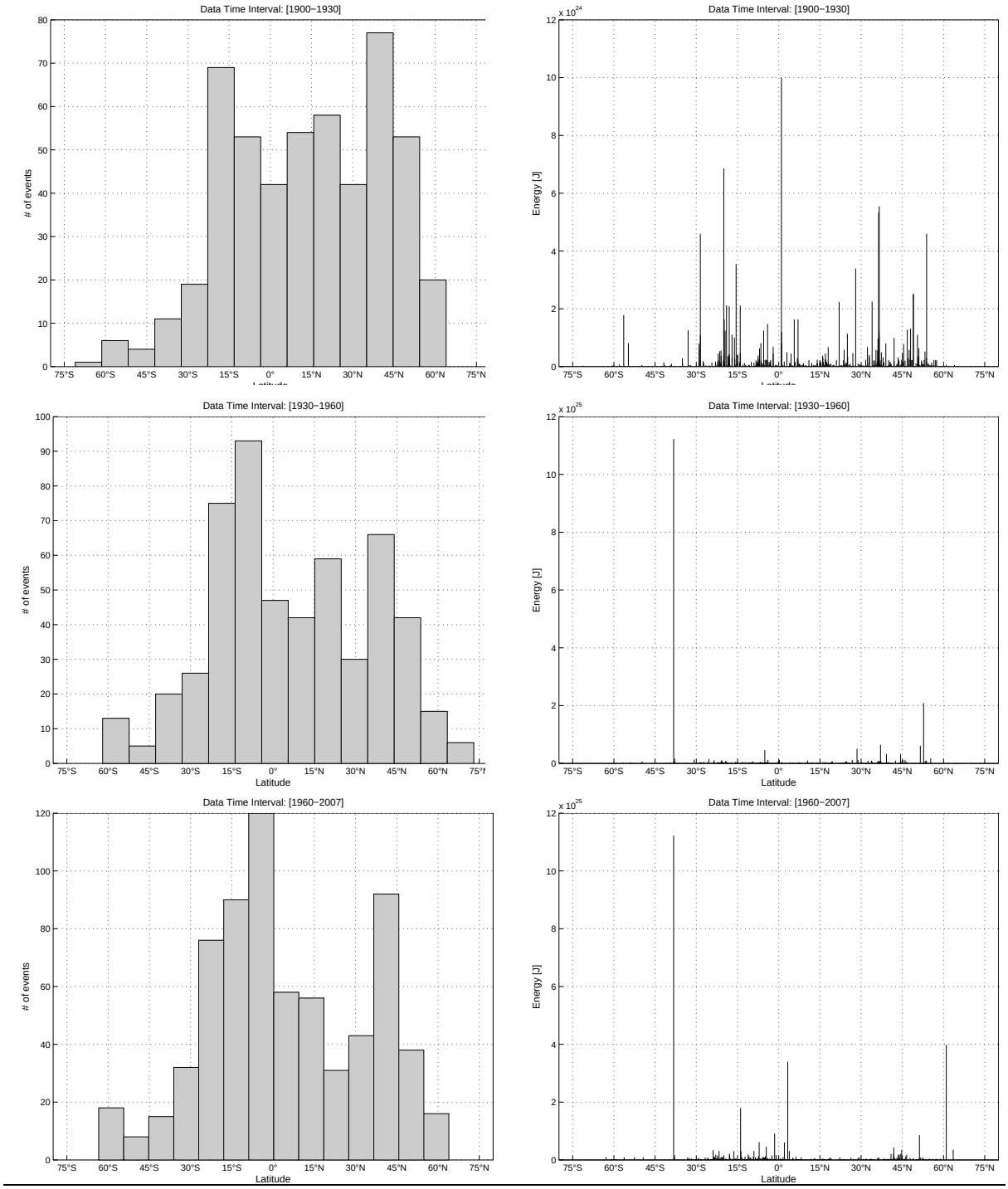

Figure 1b: along latitude

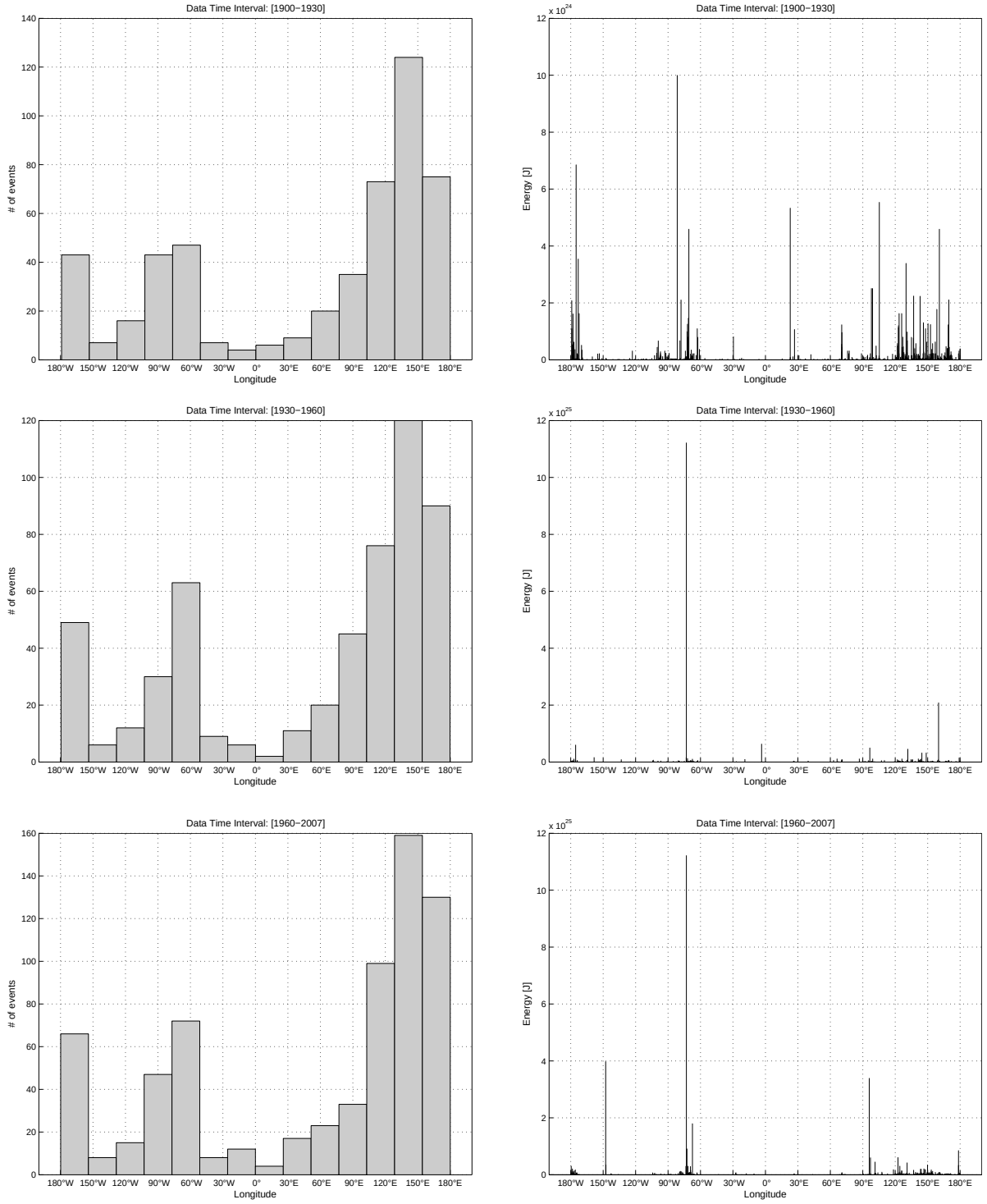

Figure 1c: along longitude

Figure 1: Distribution of the number and energy of earthquakes $M_W \geq 7.0$ along radius (a), latitude (b) and longitude (c) for time intervals 1900-1930, 1930-1960 and 1960-2007

Figure 1 shows, for the time intervals 1900-1930, 1930-1960 and 1960-2007, the distribution, of the earthquakes with $M_W \geq 7.0$, along Earth radius, latitude and longitude of the number, N, and energy,

E. If the assumption is made that the global seismicity with $M_W \geq 7.0$ is stable during the whole 20th century, from the figure it is reasonable to conclude that geographical coordinates and focal depths are determined with sufficient accuracy since the beginning of the 20th century (the histograms of N are similar in all three investigated time intervals), but the magnitudes are determined with sufficient accuracy only since the middle of XXth century
(the distribution of E in the time interval 1901-1950 is totally different from those in later periods). Therefore, in the following, only the data from 1950 to 2007 are considered.

3. Length of subduction zones and *N* in equal area latitude zones

The geographic reference for our investigations is shown in Figure 2, which is taken from the Northern Arizona University (http://jan.ucc.nau.edu/~rcb7/paleogeographic.html: Present Epoch): the solid lines have been digitized and adjusted for perspective distortion of the image. Since the original map shows the Earth in the well-known Mollweide projection (Grafarend and Krumm, 2006, p. 296 and Snyder and Voxland, 1989) the geographic coordinates latitude φ and longitude λ of the subduction zones can be easily derived from the inverse mapping equations

$$\varphi = \arcsin\frac{2t + \sin 2t}{\pi}, \quad \lambda = \frac{\pi x}{2\sqrt{2}R\cos t}, \quad t = \arcsin\frac{y}{\sqrt{2}R}$$

where x and y are the digitized coordinates. The radius R of the Earth can be eliminated during the calibration procedure in favor of the digitized coordinates of the rectangle surrounding the globe, i.e. $x(\lambda=\pm\pi,\varphi=0)$ and $y(\lambda=0,\varphi=\pm\pi/2)$. Finally, the discrete points of the subduction zones are connected by geodetic arcs (great circle arcs on the sphere) the sum of which provides a good estimate for the subduction zone length, within the specified latitude range.

4. Latitudinal distribution of *E* for seismic events with $M_W \geq 7$ and lengths of subduction zones

A significant amount of papers that characterize the latitudinal distribution of N (e.g. Chouhan and Das, 1971; Levin and Chirkov, 2001; Levin and Sasorova, 2009) and E (e.g. Sun, 1992;
Varga, 1995; Shanker et al., 2001; Denis et al., 2002) have been published. They all agree that (a) practically no significant seismic activity exists beyond latitudes ±65°, (b) the distribution of seismic energy has a zonal character (there is a maximum at the equator and two others close to ±45° latitude, fig.3b) and (c) the axial symmetry attests a possible external source influencing the global seismicity, as defined by earthquakes with $M_W \geq 7$.
Here we analyse in some detail the following properties of seismicity:

- the latitudinal distribution of strong events ($M_W \geq 7$),
- the correspondence between the latitudinal distribution of deep and shallow earthquakes and subduction zones,
- the differences between the latitudinal distribution of deep and shallow earthquakes,
- the possible effect of Earth flattening variations due to despinning (increase of length of day -LOD-) on seismic event distribution.

The basic ingredients of this analysis are: (a) the earthquake catalog for $M_W \geq 7$ for the period 1950-2007 (see section 2), (b) the tectonic data-base of subduction zone length (see section 3). From Figure 3 it is evident that the global seismic activity with $M_W \geq 7$ is mostly concentrated in shallow focus events. There is no connection in the latitudinal distribution of energy released by shallow and deep focus earthquakes.

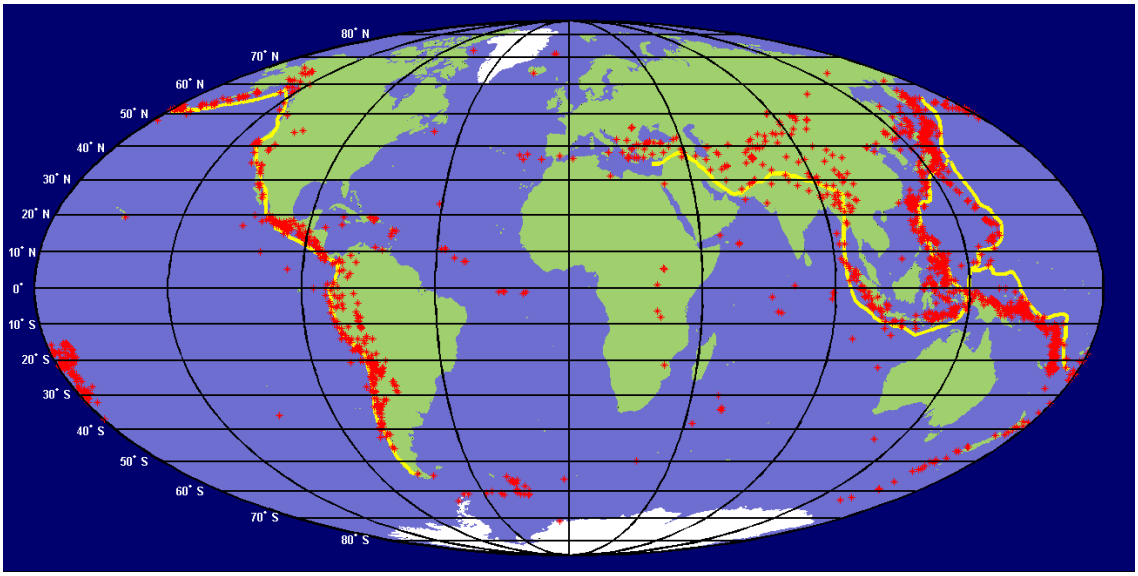

Figure 2. Map used for the determination of the length of subduction zones and number, N, of earthquakes with $M_W \geq 7$ in equal area latitude zones. Crosses denote the earthquakes listed in the catalog of seismic events of magnitudes $M_W \geq 7$, lines show the position of subduction zones where the great seismic events are generated. (Source for tectonic data: http://jan.ucc.nau.edu~rcb7/palaeographic.html)

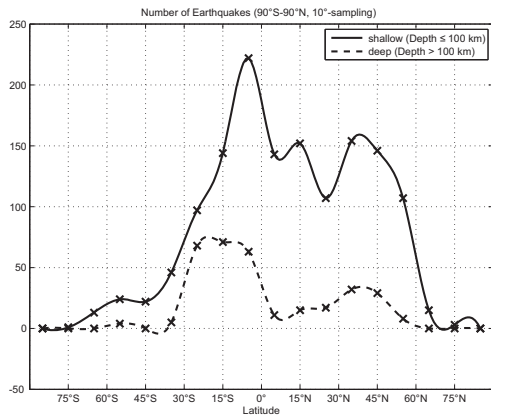

a)

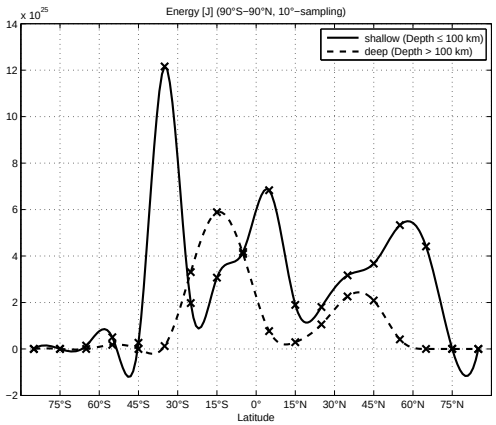

b)

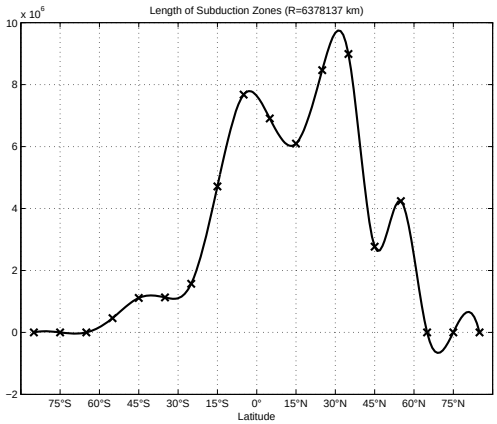

c)

Figure 3: Latitudinal distribution of seismic and tectonic activity

a- earthquake numbers along latitude (shallow and deep earthquakes)

b- earthquake energy (in Joule) along latitude (shallow and deep earthquakes)

c- *total length of subduction zones along latitude (in m)*

It is also ascertainable that along latitude there is no correlation among the distribution of *N*, *E* and length of subduction zones. From Figure 3a it is evident that *N* follows different distributions in the case of shallow and deep focus earthquakes. Probably the most important phenomenon is shown on Figure 3b: the distribution of *E* besides the equatorial extreme has maxima around latitudes ±45°. This distribution is quite coherent with the shape of the tectonic equator (TE) proposed by Crespi et al. (2007). The TE is the ideal line (great circle) describing the trajectory of the fastest westerly polarized net rotation of the mean lithosphere relative to the mantle. The TE is consistent with the asymmetric pattern of world tectonic features and tectonic plates, rather than a chaotic pattern, following a global flow of motion along TE, with an angular velocity of 1.2036° Myr. The pole of rotation of TE is at about 56.4°S and 136.7°E (Crespi et al., 2007). With reference to the TE, whose position is close to the projection of the Moon revolution orbit on the Earth's surface (Riguzzi et al., 2010), E peaks at about -5°, –35°, 20° and 45° (Figure 4).

To clarify the nature of the maxima in *E* at mid-latitudes two questions should be answered:

1. are these maxima real or are they due to the method of representation?
2. if the portrayal is objective what can be the theoretical basis of the observed phenomenon?

To answer the first question we plotted the data in Figure 5 applying different sampling rates (5°, 10° and 20°) and shifts of the coordinates (2.5°, 5° and 10°). The maxima of *N* and *E* (Figures 5a and b) are stable, while the shape of the curves of the total length of the subduction zones (Figure 5c) varies significantly (i.e. it is sensitive to the sampling rate).

We compute the distributions of *N* and *E* relative to TE, as well.

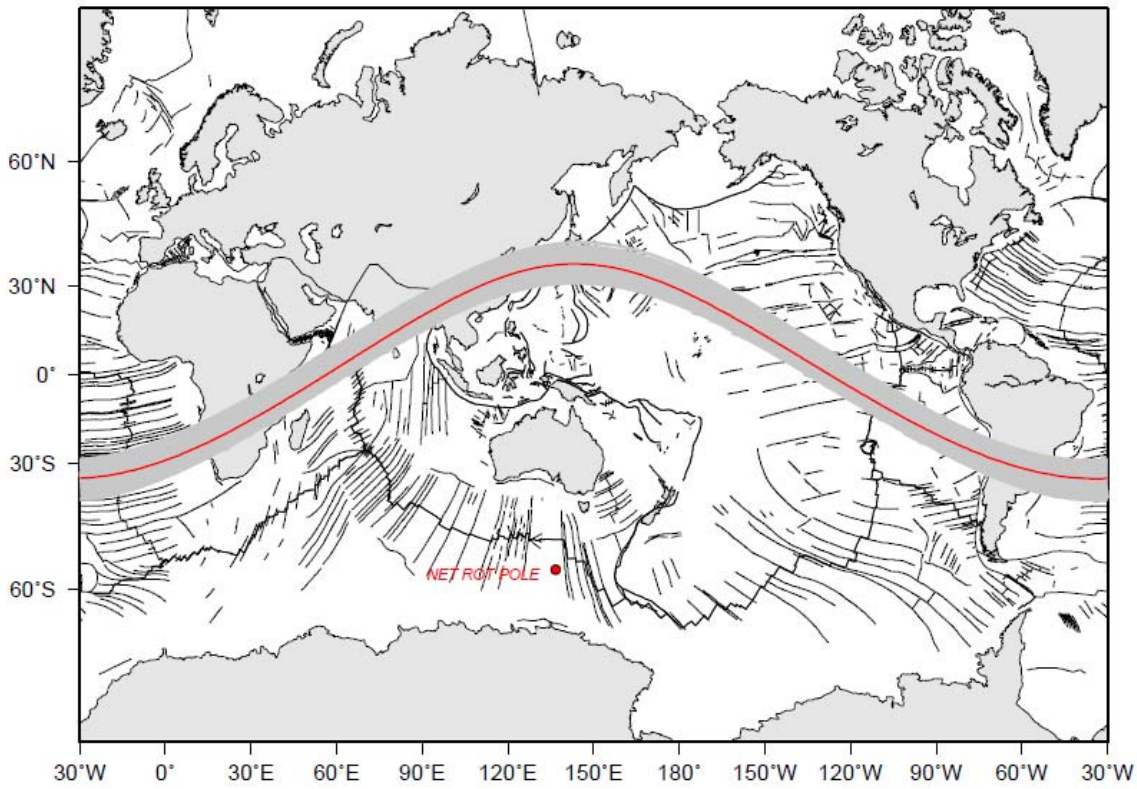

Figure 4. The net rotation equator within the tectonic mainstream latitude band where the average "westward" drift of the lithosphere relative to the mantle is faster (Crespi et al., 2007). Consistent with the present-day Vs resolution, it has been possible to define a TE-perturbed (which is not a great circle) which describes the trajectory along which an ubiquitous LVZ about 1000 km wide and about 100 km thick occurs in the asthenosphere, where the most mobile mantle LVZ is located (Panza et al., 2010).

The Gutenberg–Richter law mentions that large magnitude ($M_W \geq 7$) earthquakes are rare events, thus the energy released by one big earthquake may deplete temporally the energy budget of plate tectonics, i.e. a slab interacting with the surrounding mantle is not an isolated system, but it participates to a global expenditure of the stored energy. Therefore, the Gutenberg–Richter law supports the idea that the whole lithosphere is a self-organized system in critical state, i.e., a force is acting contemporaneously on all plates and distributes the energy over the whole lithospheric shell, a condition that can be naturally satisfied by a force acting at the astronomical scale. Plate tectonics is a global scale process and the energy source for its existence is not concentrated in limited zones (e.g., subduction zones), but it acts contemporaneously all over the whole Earth's lithosphere, like the Earth's rotation. Romashkova (2009) showed that the seismicity of the entire planet supports the idea to consider the Earth's lithosphere as a single whole system. Only the global seismicity follows the Gutenberg–Richter law, while this simple SOC relation does not hold when considering smaller portions of the Earth (Molchan et al., 1997). All these evidences and models are in favor, even if not conclusive, of a significant contribution of the Earth's rotation and of the Earth-Moon relative motion to plate tectonics.

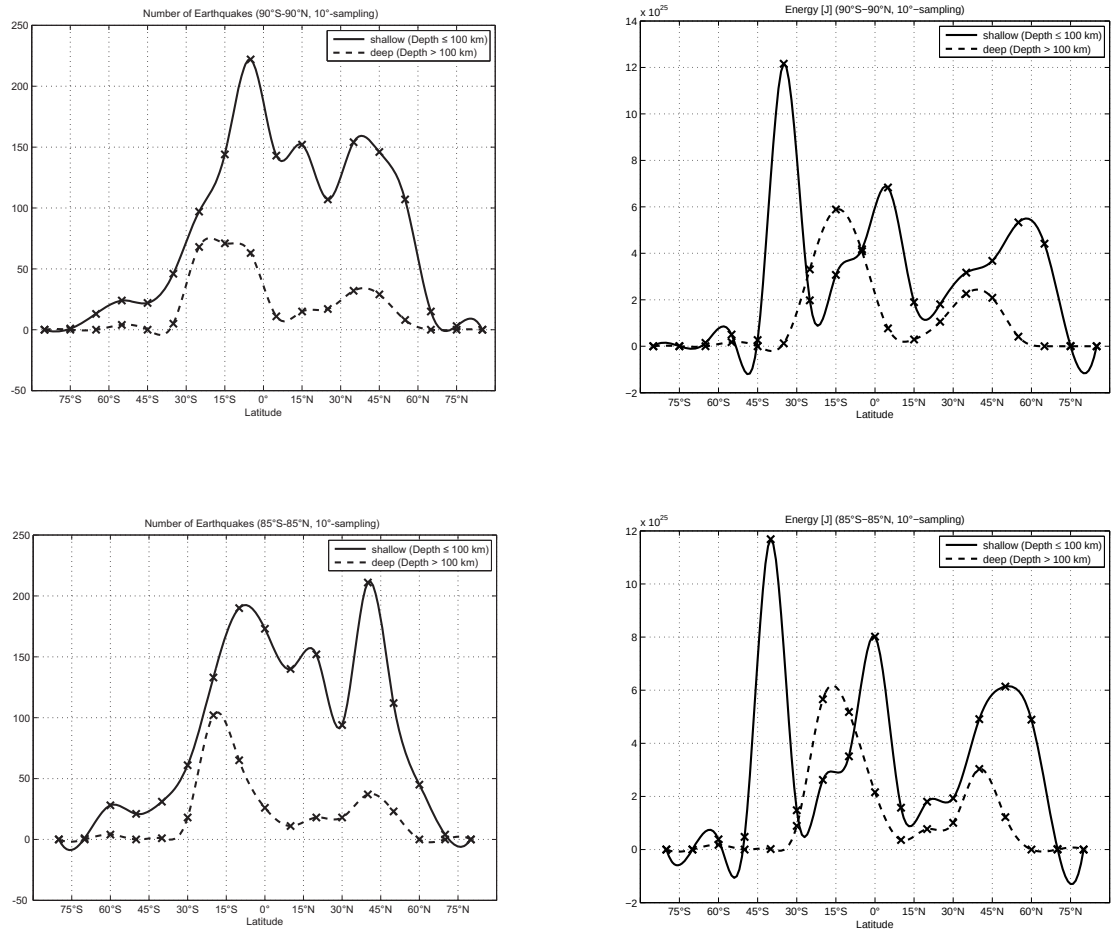

a- *sampling rate 10° without shifting (top) and with latitude shifting by 5° (bottom)*

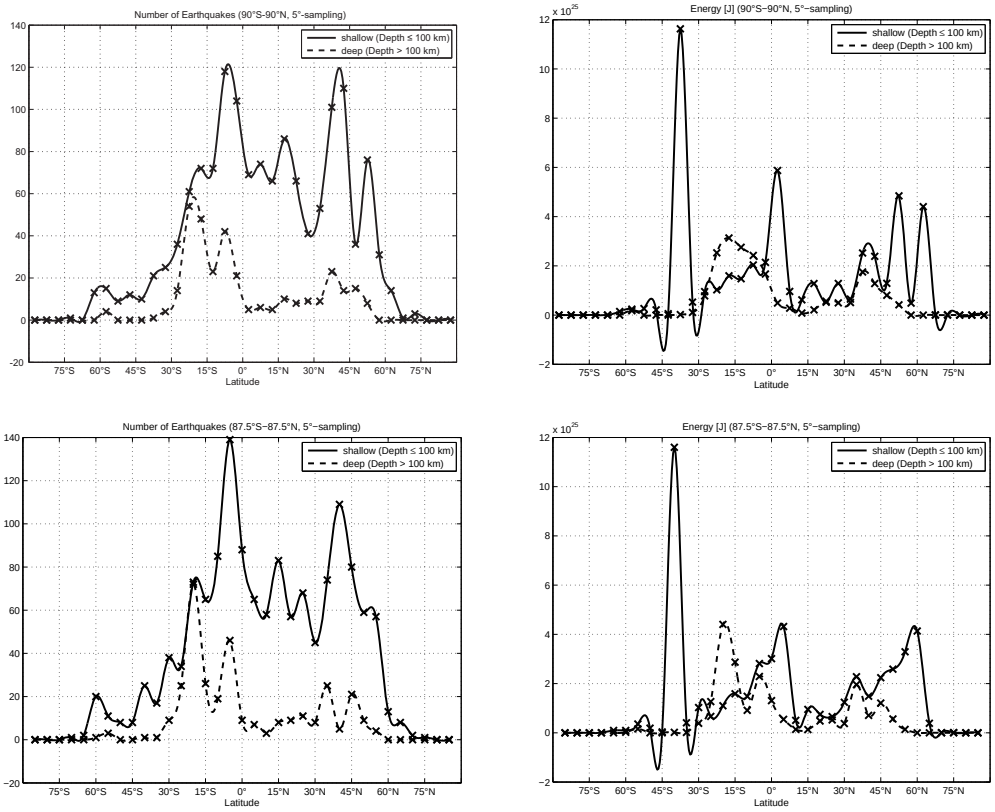

b- *sampling rate 5° without shifting (top) and with latitude shifting by 2.5° (bottom)*

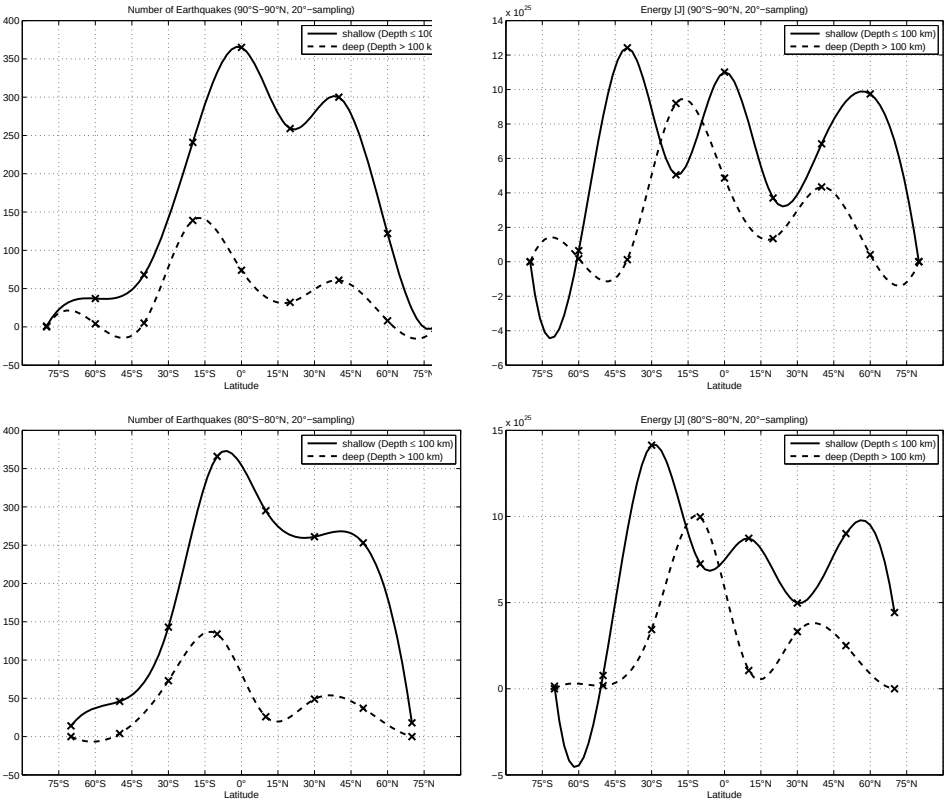

c- *sampling rate 20° without shifting (top) and with latitude shifting by 10° (bottom)*

Figure 5: Objectivity verification of graphical representation of seismicity and tectonic activity along latitudes through different sampling rates and latitude shifts

5. Influence of Earth's despinning, due to tidal friction, on global seismicity

In order to answer the second question posed in section 4, we are looking for an explanation of the phenomenon shown in Figure 3. Global regularities (axial symmetry, distribution along meridians) in the distribution of E require the presence of external long-term force acting on the Earth. The phenomenon, which can serve as an appropriate mechanism, is the decrease of the axial rotation speed due to tidal friction. Riguzzi et al. (2010) formulate the hypothesis that a significant portion of despinning energy due to tidal friction is converted into tectonic energy, as it is manifested in the latitudinal distribution of seismic energy released by earthquakes with $M_W \geq 7.0$. The variation of the flattening (Δf) of the Earth due to the linear decrease of the Earth's angular velocity is given by (Denis et al., 2002):

$$\Delta f = (1 + k_s)\frac{R}{GM}\omega\frac{d\omega}{dt}$$

Here k_s is the secular Love number (~0.96), G, M and R are the gravitational constant, the Earth's radius and mass, respectively, while ω indicates the angular speed. Amalvict and Legros (1993) have derived the formulae for the incremental meridional and azimuthal lithospheric stresses due to Δf caused by variations of angular speed:

$$\sigma_{\varphi\varphi} = -\frac{\mu\Delta f}{11}\left[5 - 3\cos 2\varphi - 4\varepsilon(3 + 7\cos 2\varphi)\right]$$

$$\sigma_{\lambda\lambda} = +\frac{\mu\Delta f}{11}\left[1 + 9\cos 2\varphi - 4\varepsilon(5 + \cos 2\varphi)\right]$$

where μ is the effective shear modulus, φ and λ are the latitude and longitude, ε is the normalized thickness of the brittle lithosphere which encompasses a soft inelastic mantle.

Consequently the resulting incremental stress difference is

$$\Delta\sigma = \sigma_{\varphi\varphi} - \sigma_{\lambda\lambda} = +\frac{\mu\Delta f}{11}(6 - 32\varepsilon)\cdot(1 + \cos 2\varphi)$$

The calculated meridional, azimuthal and resulting incremental stresses have their inflection at the critical latitudes φ=±45°, which means that the maxima of the force components $\partial\sigma_{\varphi\varphi}/\partial\varphi$ and $\partial\sigma_{\lambda\lambda}/\partial\varphi$, being proportional to the corresponding force components F_φ and F_λ, occur at these latitudes. The existence of critical latitudes can be explained as follows. A circle $A_C=4\pi R^2$ and an ellipse $A_E=\pi ab$ with equal area, $A_C=A_E$, and with coinciding centres intersect at the latitudes $\pm\varphi = \arctan\sqrt{\frac{b}{a}}$. If $a>b$ and a-b are small then we have ±φ≈45°, also called critical latitudes. Practically, the same critical latitude value holds in the case of the intersection of two arbitrary ellipses if the value of their flattening $f = \frac{a-b}{a}$ is small. Due to the action of the tidal friction, the Earth is a de-spun planet, so that f is decreasing with increasing time. Therefore, zonal areas are increasing for latitudes $\pm\varphi \geq 45°$ and decreasing for $\pm\varphi \leq 45°$.

The bimodal distribution of E, in the case of shallow events, is well recognizable in Figure 3b. It is also verifiable that the distribution of E, in the case of deep and shallow earthquakes foci is quite different. Similarly significant difference in latitudinal distributions can be observed between E and the global linear tectonic structures (compare Fig. 3b and 3c). The clear latitude dependence of earthquake energy release and its symmetry relative to the axis of rotation suggests that an external component, the tidal friction, influences the tectonic processes through the generated variations of the hydrostatic figure of the Earth.

6. Depth distribution of earthquake energy

The earthquake process transfers the potential energy stored in form of stress in rocks to elastic wave, rupture and heat energy (Kanamori, 2001). The real amount of energy accumulated in rocks is not known, due to the uncertainty about the radiation efficiency mainly of deep earthquakes. The

efficiency, i.e. the ratio of radiated energy to the potential one, has been rather low, in comparison with shallow focus events, in the case of some deep focus events, like the deepest big event in Bolivia (1994, h = 631 km, $M_W = 8.2$), or the 1999 China-Russian border earthquake (h = 566 km, $M_W = 7.1$) where a significant part of the accumulated energy has been converted into heat (Venkataraman and Kanamori, 2004).

It is well known that N decreases with increasing depth as $\sim 1/h$ (where h is the focal depth expressed in km) up to the depth of 300 km. Only 25% of all earthquakes have reported focal depths exceeding 60 km (Frohlich, 2006). The depth distribution of E (Figure 1a) is not uniform. The preponderant part of energy (90%) is concentrated in the crust (3×10^{26} Joule/year) with a sharp maximum at the depth around 30 km (33 km is a quite popular, default value for shallow events). A large anomaly of E (about 4×10^{25} Joule/year) distribution is due to 57 events which occurred between 1950 and 2007 in the depth range from 550 to 680 km.

Clustering of earthquake energy release at this depth interval was detected and described a long time ago in different contributions by Gutenberg and Richter (1936, 1938, 1939, 1942, 1954 and 1956).

Not all subduction zones characterized by high seismic energy radiation at shallow focus ($h \leq 50$ km) are connected to deep earthquake energy sources. As can be seen from Figure 6a, lithospheric slabs penetrating into the mantle in Central America, Barbados, Aleutians and east from New Zealand are characterized mainly by shallow focus earthquakes.

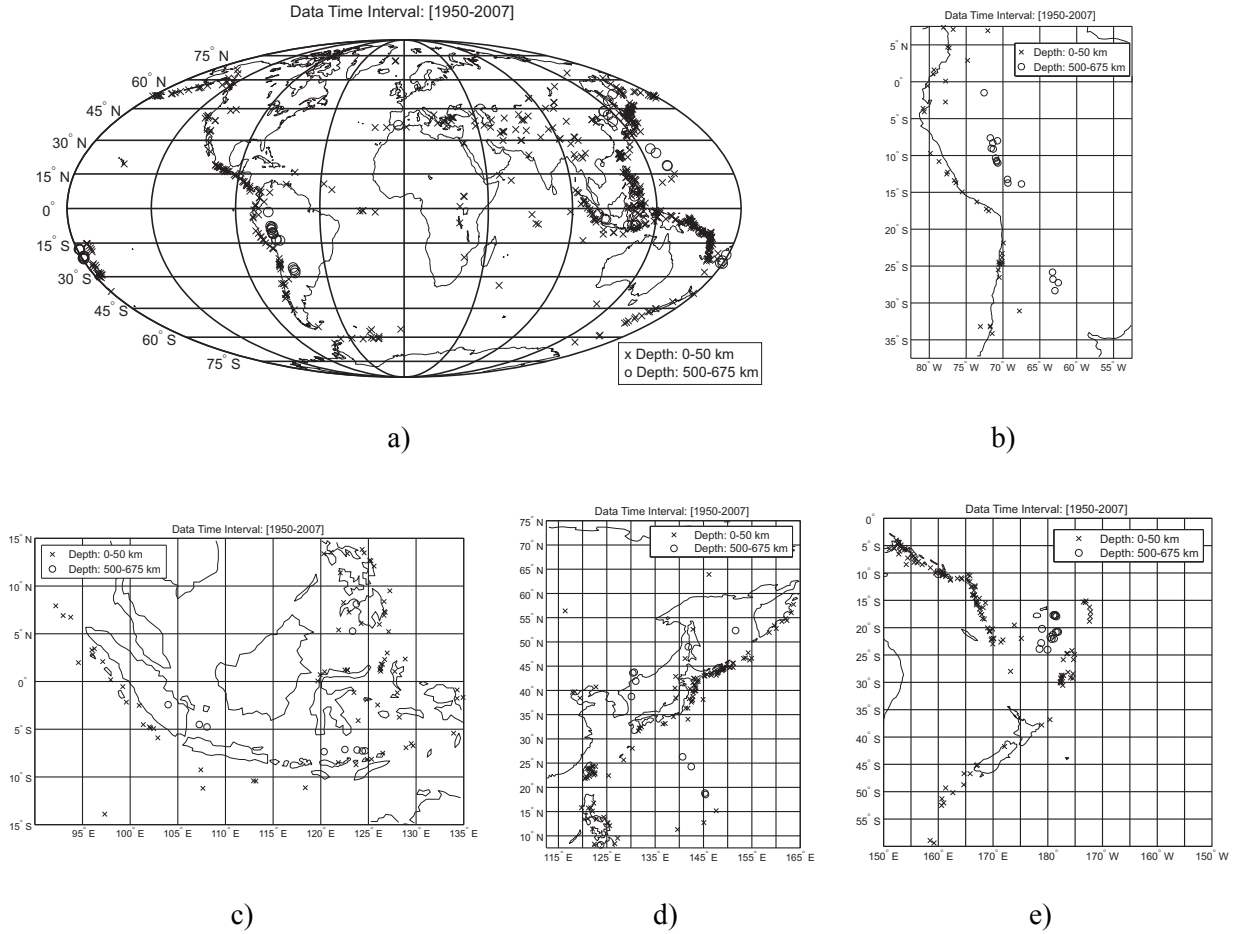

Figure 6: Distribution of shallow (depth interval 0-50 km) (×) and deep (depth interval 550-680 km) (O) focus earthquakes

- *a- global map*
- *b- West South America (Peru and Chile subduction zones)*
- *c- Indonesia (Sumatra, Banda sea and East Luzon or Philippine subduction zones)*
- *d- Japan-Kuriles subduction zones*
- *e- Kermadec-Tonga subduction zones*

On the other hand, the subduction zones of the Pacific coast of South America between latitudes 10°S and 30°S (slabs in Peru-Bolivia and Chile) (Figure 6b), the slabs of South Asia (Sumatra, Banda Sea and Timor, Philippine and East Luzon) (Figure 6c), Kermadec Island area (Figure 6e) and the slabs in the vicinity of Japan, Kuriles and Kamchatka (Figure 6d) are marked both by shallow and deep earthquake sources ($h \geq 500$ km).
In the source areas where shallow and deep focus earthquakes occur, two angles can be identified: slab dip β taken from Riguzzi et al. (2010) and the angle α between the surface and the straight line connecting shallow and deep source zones (average dip). (Fig. 7). We find (Table 1) in the case of the E-directed slabs of South America $\alpha = 50°$, while the typical slab dip β in this region, for $h > 70$ km, is $\beta = 20°$.

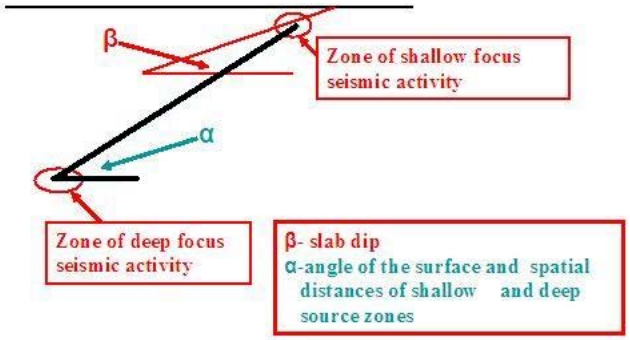

Fig. 7. Angle of the surface and spatial distances of shallow and deep source zones (α) and slab dip (β)

Subduction zones with deep earthquake activity	$\alpha°$	$\beta°$
Peru	49	15
Chile	54	23
Sumatra	60	32
Banda Sea (Timor)	74	55
Philippine (East Luzon)	66	63
Japan	42	35
Kuriles - Kamchatka	45	45
Kermadec Islands	55	58

Table 1. Angles of the surface and spatial distances of shallow and deep source zones (α) and slab dips β

Similar values are observed in the Sumatra source zone (NE-directed slab). This means that typically $\alpha - \beta \approx 30°$ and the Benioff-Wadati zones consisting of both shallow and deep source zones (Figures 6b, 6c) are not straight and this may imply that there is no direct relation between the two active zones. For the W-oriented slabs the situation is different. In Southern Asia (Banda Sea-Timor, Philippine -East Luzon, Figure 6c), in the Far East (Figure 6d), Japan and Kuriles–Kamchatka source zones and Kermadec Islands (Figure 6e) we get

smaller values for α - β, averaging at about 6°, even when the α values are close to the case of the E-oriented slabs. This means that the Benioff-Wadati zones are not bent in these cases. In other words, the deep seismicity along W- or SW-directed slabs is regularly connected to the superficial part of the subduction zone (α - $\beta \approx 6°$), while along E- or NE-directed subduction zones the large difference between dips (α - $\beta \approx 30°$) rather suggests a different origin of the deep seismicity. In fact, along these subduction zones, the seismicity is very low or absent between 300 and 550 km of depth (Riguzzi et al., 2010) and the deep seismicity may have the following origin. Instead of common interpretation of a slab, it can be related to a mantle suction process and to the shear between upper and lower mantle generated by a sort of Venturi effect: the mantle, in correspondence of E- or NE-directed subduction zones, can flow through a surface that is significantly reduced, with respect to standard situations, by the subduction plate marked by seismicity not deeper than about 300 km. Therefore the deep earthquakes along the E- or NE-directed slabs may be related to the subduction system, which is sucking up the mantle, but they occur in the mantle without requiring the presence of any slab (e.g., Doglioni et al., 2009). The only exception is the Kermadec Islands zone where, between 1950 and 2007, 16 earthquakes with $M_W \geq 7.0$ were detected in the depth range from 350 km to 450 km.

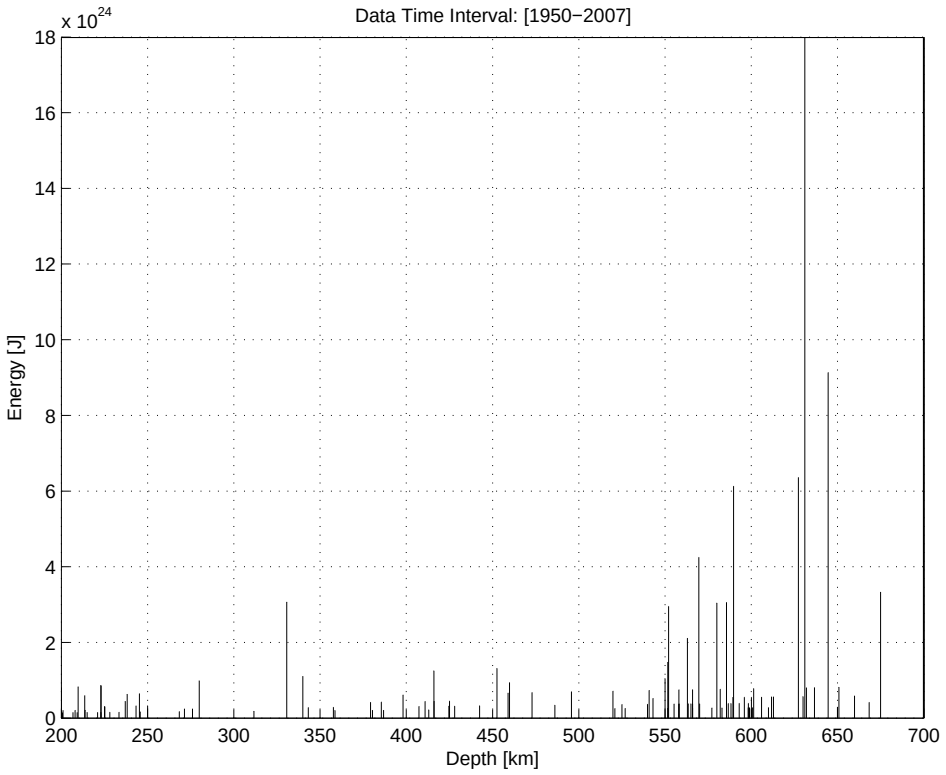

Figure 8: Earthquake energy released at of depth interval 200-680 km

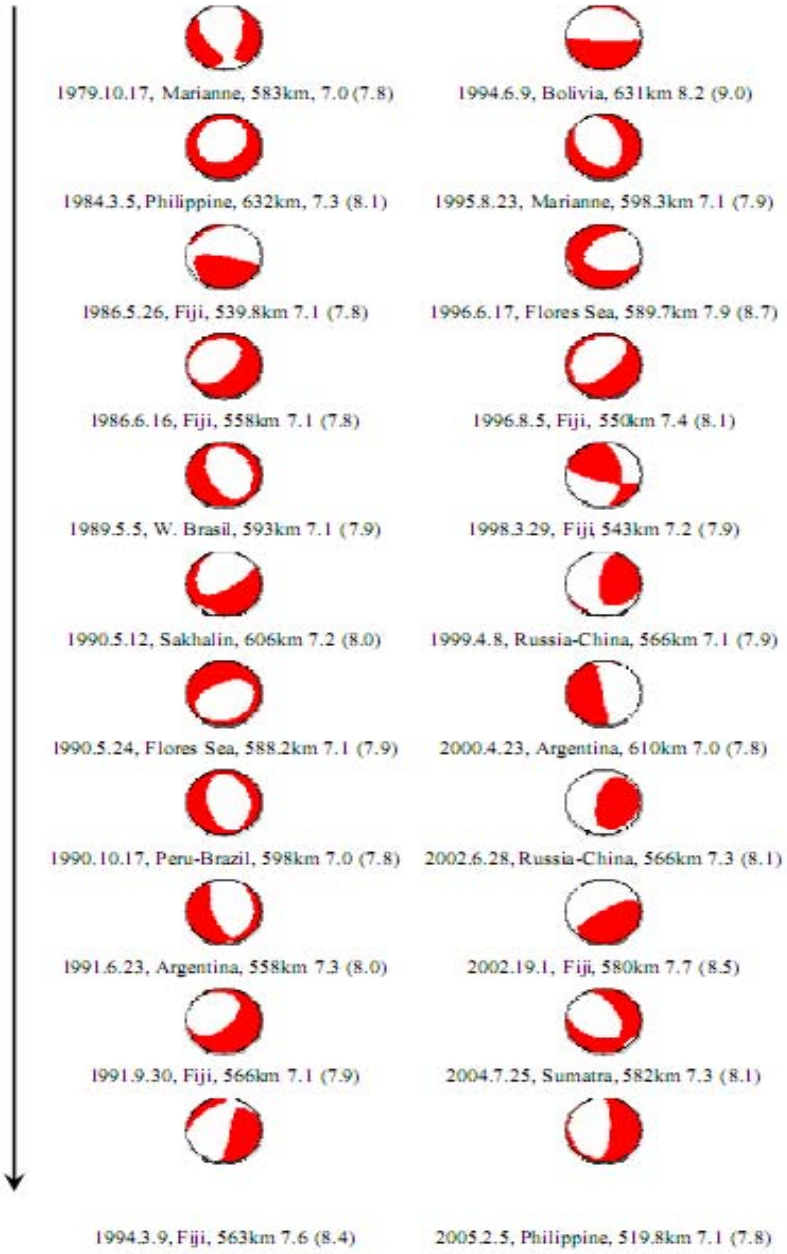

Figure 9: Focal mechanisms for earthquakes $M_W \geq 7.0$ for time interval 1979-2005in the vicinity of the bottom of the transition zone (depth interval 600-680 km). M_W values of Engdahl and Villaseñor, 2002 (and corrected according Herak et al., 2001)

Most of the elastic energy radiated by deep events is concentrated in the depth interval between 580 km and 640 km (Figure 8), somewhat above the lower border of the transition zone given in PREM. Green (2007) proposed that deep earthquakes are related to shearing instabilities accompanying high-pressure phase transformations. Most of the 27 focal mechanisms given in the Harvard CMT Catalog for the deep events with $M_W \geq 7.0$ occurred in the time interval 1976-2005 have a major extensional component (Figure 9), well consistent with an accelerated mantle flow through narrow structures (e.g. Hilst, 1995) across the lower boundary of the C layer. This phenomenon leads to the reduction in pressure (Venturi effect) what is reflected in the extensional

character of the focal mechanism of the earthquakes with $M_W \geq 7$ which occurred, in depth interval from 520 km to 630 km, close to the bottom of the transition zone.
According to Kirby et al.,1996 and Venkataraman & Kanamori, 2004 the intra-slab seismicity is restricted to the cold cores of the slabs and is mostly in down-dip compression along W-directed subduction zones, whereas it is mostly a down-dip extension along the opposite E- or NE-directed subduction zones (Doglioni et al., 2007). These global scale asymmetries of subduction zones associated to those observed along oceanic ridges (Panza et al., 2010) support the notion of the net-rotation of the lithosphere, which is moving westerly relative to the underlying mantle much faster than previously estimates (Crespi et al., 2007).

7. Conclusions

In our study we used earthquake energy release data derived from a global earthquake catalog of events with $M_W \geq 7.0$. A careful analysis of the available data shows that only the time interval from 1950-2007 is suitable for our purposes.
The surface distribution of E has axial symmetry and it indicates the presence of an external stress-generating force that is reasonable to associate with tidal effects. The energy dissipation due to tidal friction is around $1.6 \cdot 10^{19}$ Joule/year, while the radiated earthquake energy is $9.5 \cdot 10^{18}$ Joule/year (Riguzzi et al., 2010). The energy generated by the despinning of the Earth is converted into elastic energy by means of deformation of the brittle outermost part of the Earth in the vicinity of the critical latitude, first of all due to the attenuation of geometrical flattening, as it has been shown earlier by Varga et al. (1997) (during the Phanerozoic the value of flattening has changed by as much as 36%).
The depth distribution of energy has two peaks: the most important, which represents ~90% of the seismic energy released is connected with the seismicity of the brittle crust (~30 km); the other is situated at the lower boundary of the transition zone between upper and lower mantle (responsible for ~10% of earthquake energy).
The deep seismicity along W- or SW-directed slabs is regularly connected to the superficial part of the subduction zone ($\alpha - \beta \approx 6°$), while along E- or NE-directed subduction zones the large difference between dips ($\alpha - \beta \approx 30°$) rather suggests a different origin of the deep seismicity. Along these subduction zones, the deep seismicity rather than due the presence of a slab, can be related to mantle shear between upper and lower mantle generated by a sort of Venturi effect: the mantle, in correspondence to E- or NE-directed subduction zones, can flow through a surface that is significantly reduced, with respect to standard situations, by the subduction plate marked by seismicity not deeper than about 300 km. Therefore the deep earthquakes along the E- or NE-directed slabs may be related to the subduction system, which is sucking up the mantle, but they occur in the mantle without requiring the presence of any slab (e.g., Doglioni et al., 2007; Doglioni et al., 2009). The shallow release of energy could possibly be related chiefly to the lower temperature, controlling brittle failure. However, it could also be an indication of the larger shear exerted in the shallow Earth by the solid tide. Moreover, the observation that most of the energy is released in the first 30 km or so would prove that the slab pull may not be the main driving force for moving plates.

Acknowledgements

This paper was partly completed in the framework of the bilateral project DFG-HAS 189 ("Study of the time dependent geophysical and geodetic processes"). Financial support from the Hungarian Science Found OTKA Project K84072 and MIUR COFIN 2008 is acknowledged.

References

Abe K., Noguchi S., 1983. Revision of magnitudes of large shallow earthquakes, 1897-1912, Phys. Earth Planet. Int., 33, 1-11

Amalvict M., Legros H., 1993. Stresses int he lithosphere induced by the Earth rotation, In: Physics and Evolution of the Earth's Interior, volume 6: Dynamics of the Earth's Evolution, ed. R. Teisseyre, 348-349, PWN Warszawa and Elsevier, Amsterdam

Chouhan R.K.S., Das U.C., 1971. Preliminary report on global seismicity-frequency energy distribution of earthquakes, Pure Appl. Geophys., 89, 1, 98-108

Crespi M., Cuffaro M., Doglioni C., Giannone F., Riguzzi F., 2007. Space geodesy validation of the global lithospheric flow. Geophys. J. Int., 168, 491-506, doi: 10.1111/j.1365-246X.2006.03226

Denis C., Schreider A.A., Varga P., Závoti J., 2002. Despinning of the Earth rotation in the geological past and geomagnetic paleointensities, J. Geodyn., 34, 5, 97-115

Doglioni C., Carminati E., Cuffaro M. and Scrocca D. 2007. Subduction kinematics and dynamic constraints. Earth Sci. Rev., 83, 125-175, doi:10.1016/j.earscirev.2007.04.001

Doglioni C., Tonarini S., Innocenti F., 2009. Mantle wedge asymmetries along opposite subduction zones. Lithos, 113, 179-189, doi:10.1016/j.lithos.2009.01.012

Engdahl, E.R., Villaseñor A., 2002, Global Seismicity. 1900–1999, in W.H.K. Lee, H. Kanamori, P.C. Jennings, and C. Kisslinger (editors), International Handbook of Earthquake and Engineering Seismology, Part A, Chapter 41, pp. 665–690, Academic Press

Frohlich C., 2006. Deep earthquakes, Cambridge University Press

Galitzin, B.B., 1915. Sur le tremblement de terre du 18 février 1911, Comptes Rendus, 160, 810-813 (paper was reproduced without any omission in Klotz, 1915)

Grafarend E.W., Krumm F.W., 2006. Map projections, Cartographic Information System, Springer, 713 pages

Green H.W., 2007. Shearing instabilities accompanying high-pressure phase transformations and the mechanics of deep earthquakes. Proc. Nat. Ac. Sci. USA, doi_10.1073/pnas.0608045104

Gutenberg B., Richter C.F., 1936. Materials for the study of deep-focus earthquakes, Bull. Seism. Soc. Am., 26, 4, 341-390

Gutenberg B., Richter C.F., 1938, 1939. Depth and geographical distribution of deep-focus earthquakes, GSA Bulletin. 49, 1, 249-288; 50, 1511-1528

Gutenberg B., Richter C.F., 1942. Earthquake magnitude, intensity, energy, and acceleration, Bull. Seism. Soc. Am., 32, 163-191

Gutenberg B., Richter C.F., 1954. Seismicity of the Earth, Princeton University Press, 2nd edition

Gutenberg B., Richter C.F., 1956. Earthquake magnitude, intensity, energy and acceleration (second paper), Bull. Seism. Soc. Am., 46, 105-145

Hanks T.C., Kanamori H., 1979.A moment magnitude scale, J. Geophys. Res., 84, B5, 2348-2350

Herak, M., Panza, G.F., Costa G., 2001. Theoretical and observed depth correction for M_S. Pure Appl. Geophys., 158, 1517-1530

Hilst van der, R. D. 1995. Complex morphology of subducted lithosphere in the mantle beneath the Tonga trench, Nature 374: 154–157

Howell B.F.Jr., 1990. An introduction to seismological research. History and development, Cambridge University Press

Jeffreys H., 1923. The Pamir earthquake of 1911, February 18, in relation to the depths of foci. Mon. Not. Roy. Astr. Soc., Geophys. Suppl., I, 22-37

Kanamori, H., 2001. Energy budget of earthquakes and seismic efficiency, in Teisseyre, R., and Majewski, E., eds., Earthquake Thermodynamics and Phase Transformations in the Earth's Interior, Academic Press, 293-305

Kirby, S. H., Stein S., Okal E. A., Rubie D. C., 1996. Metastable mantle phase transformations and deep earthquakes in subducting oceanic lithosphere, Rev. Geophys., 34, 2, 261-306

Klotz, O., 1915. Earthquake of February 18, 1911, Bull. Seism. Soc. Am., 5, 206-213

Kosobokov V. G., 2004. Earthquake prediction: basics, achievements, perspectives, Acta Geod. Geophys. Hung., 39, 2-3, 205-221

Kövesligethy R., 1897. Neue geometrische Theorie seismischer Erscheinungen, Mathematische und Naturwissenschaftliche Berichte aus Ungarn, XIII

Kövesligethy R., 1903. Über die Energie großer Erdbeben, Die Erdbebenwarte Monatsschrift, III. Jahrg. 1903/1904, 196-202

Levin B.W., Chirkov Ye. B., 2001. Planetary maxima of the earth seismicity, Phys. Chem. Earth (C), 26, 10-12, 781-786

Levin B.W., Sasorova E.V., 2009. Latitudinal distribution of earthquakes in the Andes and its Peculiarity, Adv. Geosci., 22,139–145

Milne J., 1886. Earthquakes and other earth movements, Kegan Paul, Trench & Co., 363

Molchan, G., Kronrod, T., Panza, G.F., 1997. Multi-scale seismicity model for seismic risk. Bull. Seism. Soc. Am., 87, 5, 1220–1229.

Panza G., Doglioni C., Levshin A., 2010. Asymmetric ocean basins, Geology, 38, 1, 59-62

Reid H.F., 1912. The energy of earthquakes, Comptes Rendus des séances de la quatrième conférence de la Commission Permanente et de la deuxième assemblée générale l'Association Internationale de Sismologie, Réunies a Manchester (Ed. R. Kövesligethy), 268-274

Richter C.F., 1935. An instrumental earthquake magnitude scale, Bull. Seism. Soc. Am., 25, 1-3

Riguzzi F., Panza G., Varga P., Doglioni C., 2010. Can Earth's rotation and tidal despinning drive plate tectonics? Tectonophysics, 484, 1-4, 60-73

Romashkova, L.L., 2009. Global-scale analysis of seismic activity prior to 2004 Sumatra-Andaman mega-earthquake. Tectonophysics 470, 329–344, doi:10.1016/j.tecto.2009.02.011.

Shanker D., Kapur N., Singh V. P., 2001. On the spatio temporal distribution of global seismicity and rotation of the Earth - A review, Acta Geod. Geophys. Hung., 36, 2, 175-187

Sieberg A., 1923. Erdbebenkunde, Verlag von Gustav Fischer, Jena, 572 pages

Snyder J.P., Voxland P.M., 1989. An album of map projections, U.S. Geological Survey, Professional Paper 1453, 249 pages, United States Government Printing Office, Washington 1989

Sun W., 1992. Seismic energy distribution in latitude and a possible tidal stress explanation, Phys. Earth Planet. Int.,71, 3-4, 205-216

Varga, P., 1995. Temporal variation of the figure of the Earth and seismic energy release. Publication of the Institute of Geodesy and Navigation, University FAF, Munich, 118-127

Varga, P., Denis, C., Varga, T., 1997. Tidal friction and its consequences in paleogeodesy, in the gravity field variations and in tectonics. J. Geodyn., 251, 61-84

Venkataraman A., Kanamori H., 2004. Observational constraints on the fracture energy of subduction zone earthquakes, J. Geophys. Res., 109, B05302, doi:10.1029/2003JB002549